



Flow Characteristics of a Pipe Diffuser for Centrifugal Compressors

Z. Sun, X. Zheng[†] and Z. Linghu

Turbomachinery Laboratory, State Key Laboratory of Automotive Safety and Energy, Tsinghua University, Beijing, 100084, China.

[†]Corresponding Author Email: zhengxq@tsinghua.edu.cn

(Received April 29, 2016; accepted July 30, 2016)

ABSTRACT

The pipe diffuser, an efficient kind of radial bladed diffuser, is widely used in centrifugal compressors for gas turbine engines. This paper investigates flow characteristics of a pipe diffuser for centrifugal compressors by solving three-dimensional Reynolds-averaged Navier-Stokes equations. The results show that the pipe diffuser is adaptable to high Mach number incoming flows, and its unique leading edge could uniform the flow distortion. Numerical analysis indicates that the choke in pipe diffuser occurs suddenly, which leads to the dramatically steep performance curves near choke condition. Besides, it is found that the first half flow passage is particularly important to the pipe diffuser performance as it influences the choking behavior, the static pressure distribution, and the matching, so more attention should be paid to this region when designing or optimizing a pipe diffuser. Two counter-rotating vortices generated in the diffuser inlet region are captured by numerical simulation, and they can exist in the downstream of the diffuser passage. More detailed analysis show that these two vortices dominate the flow structure in the whole diffuser passage by shifting flow to certain positions and forming high-momentum flow cells and wake flow cells. The leading edge formed by the intersection of adjacent diffuser passages significantly affects this pair of vortices. In addition, these two vortices also affect the flow separation in pipe diffuser flow passages, they suppress separation near the front wall and back wall while facilitate separation at center locations. Therefore, it is recommended to design the leading edge of the pipe diffuser carefully to control the vortices and obtain a better flow field.

Key Words: Pipe diffuser; Centrifugal compressor; Flow characteristics; Counter-rotating vortices; CFD; Flow separation.

NOMENCLATURE

A	area	x	the abscissa of the reference frame
c_p	pressure recovery	y	the ordinate of the reference frame
l	distance from diffuser throat to diffuser outlet	y^+	non-dimensional wall distance of first node
\dot{m}	mass flow rate	Subscripts	
M_a	absolute Mach number	0	total parameter
N	rotation speed	1	pipe diffuser inlet
p	pressure	2	pipe diffuser outlet
ω	loss coefficient		

1. INTRODUCTION

Centrifugal compressors are widely used in gas turbine engines, as they can achieve high pressure ratio and enable engines to be more compact. At the same time, centrifugal compressors often suffer low stage efficiency on account of the long flow path and strengthened secondary flow phenomena, especially in diffusion components. A centrifugal compressor applied in jet engines primarily consists of two

components: the impeller and the diffuser. Researches have devoted to the design and the improvement of diffusers to obtain higher stage efficiency, and the pipe diffuser introduced by Kenny (1969) and Runstadler *et al.* (1969) turns out to be an efficient design. Compared with conventional vane island diffusers, the pipe diffuser has many advantages. Bennett *et al.* (2000) point out that the pipe diffuser has higher stage efficiency and fewer friction losses. Moreover, the pipe diffuser is able to

handle highly distorted inlet flow and gain superior performance at high inlet Mach numbers. The pioneering researches by Kenny (1969, 1970 & 1972) show that pipe diffusers have lower manufacturing cost, superior efficiency with supersonic inlet flow, and smaller throat blockage compared with alternative designs. The pipe diffuser has been applied in industrial products by General Electric and Pratt and Whitney in North America (Bennett *et al.* 2000, Kenny 1972), and it is likely to play a more important role in compressors where the Mach number is high at the diffuser inlet (Kenny 1970, Zachau 2008).

Due to the data protection for commercial security, open literature and available information about pipe diffusers are limited. Some researches are carried out to investigate the key parameters and their influences on the performance of pipe diffusers. Reeves (1977) compares the performance of pipe diffusers with different inlet cross-sections. He proposes that the incidence at the inlet could have a considerable effect on the performance of pipe diffusers, and an optimum incidence for best performance is negative 3 degrees. Researches on the pipe diffuser throat have been done by Bennett *et al.* (2000). They investigate pipe diffusers with different throat cross-sectional shapes and proposes an optimum 'side-wall expansion'. Besides, they introduce a design criterion for the throat size. The number of passages in the whole 360 degrees is another crucial parameter. The works by Groh *et al.* (1970) show that increasing the passage number of pipe diffusers extends the stable operation range without decreasing efficiency. However, the results from Bennett *et al.* (1998) suggest that pipe diffusers with a low number of passages can get wider operating range at the cost of increased unsteadiness and flow distortion. The length of the flow passage also influences the performance of pipe diffusers, and it is studied by Kunte *et al.* (2013), and they truncate the pipe diffuser and observe an increase of 0.3% in stage isentropic efficiency. Moreover, the flow angle at the pipe diffuser outlet changes when the pipe diffuser is truncated.

Some investigations are focused on the flow structures and flow characteristics of the pipe diffuser. Zachau (2008) studies the three-dimensional flow phenomena with PIV technology, and results show that streamlines are pushed to the suction side (SS) of the passage and flow separation occurs in regions near the pressure side (PS). Grates *et al.* (2014) reveal that the fluid flow inside impeller and pipe diffuser is highly unsteady. In the inlet domain, the leading edge of the pipe diffuser generates a pair of vortices, and it can help mix the non-uniform inlet flow better (Zachau 2008, Grates *et al.* 2014, and Zachau *et al.* 2009). Grates *et al.* (2014) also investigate the generation process of the vortices by unsteady CFD and notices that the intensity of the vortex near impeller hub is constant in time while the other one is oscillating.

Previous research on pipe diffusers provides useful information about the critical parameters, the flow field, and the vortices. The geometry information is introduced in some papers and patents. However, the

relationship between the flow characteristics and the geometric features of the pipe diffuser performance is unclear. In this paper, flow characteristics of a pipe diffuser for centrifugal compressors are investigated by solving three-dimensional Reynolds-averaged Navier-Stokes equations, and the underlying mechanism of the flow characteristics associated with the geometry features is revealed.

2. GEOMETRY CHARACTERISTICS

The pipe diffuser is essentially a kind of radial bladed diffuser. Its geometry and structure are similar to that of a channel diffuser or a wedge diffuser. The geometry characteristics of pipe diffusers have been described in previous studies (Kenny 1970, Reeves 1977, and Salvage 1997). An array of radial diffusion pipe passages is spaced uniformly in circumferential direction in the diffuser ring, and all centerlines of pipe passages are tangent to a common tangency circle whose diameter is substantially identical to that of the periphery of the impeller. The fluid particles leave the center region of impeller blades at angles above tangential whereas fluid particles near the front and back shrouds leave at angles quite near the tangential. Therefore, an appropriate incidence at the diffuser inlet is achievable when passage center lines are tangent to the same tangency circle. Pipe diffuser passages are made to intersect with adjacent ones and in this way the leading edges with elliptical ridges (Fig. 1) are formed (Kenny 1969, Zachau 2008, Grates *et al.* 2014, Zachau *et al.* 2009, and Kunte *et al.* 2013). At the same time, the beginning and the cusp (shown in Fig. 2) of the elliptical ridges are located in two circles outside the tangency circle, respectively. Finally, as presented in Fig. 2, three different spaces are formed between the tangency circle and the diffuser throat. Regions inside the cusp of the elliptical ridges are called vaneless space while regions outside the beginning of elliptical ridges (leading edge radius) are semi-vaneless space. Between them is the pseudo-vaneless space.

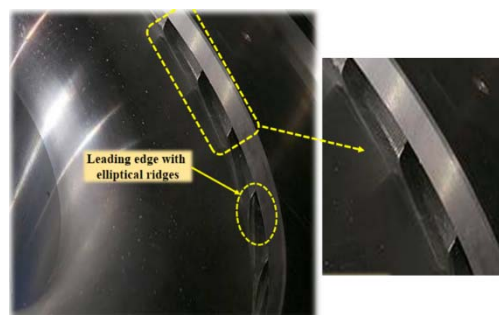


Fig. 1. The inlet region of a pipe diffuser.

Downstream of the semi-vaneless space is the throat of a pipe diffuser, a short region of constant cross-section area (shown in the enlarged view in Fig. 3). The streamwise length of the throat affects the stage performance. According to Han *et al.* (2014), increasing the throat length decreases the efficiency and pressure ratio at design point while it improves the performance at near surge point.

The diffusion law of the passage is a unique feature

of the pipe diffuser geometry. To express this law clearly, a reference frame is established as shown in Fig. 3. Its origin is located at the center point of the diffuser throat inlet, and the distance from throat inlet to diffuser passage outlet is denoted as l . Based on this frame, the distribution of the cross-section area of the diffuser passage from the throat inlet to the diffuser outlet ($0 < x/l < 1$) is displayed in Fig. 4. According to the inclination of the area distribution curve, the cross-section area increases slowly near diffuser throat but much more quickly at the rear parts. The main reason for such a diffusion law lies in the requirements of controlling reverse static pressure gradient, which is demonstrated in the later part of this paper.

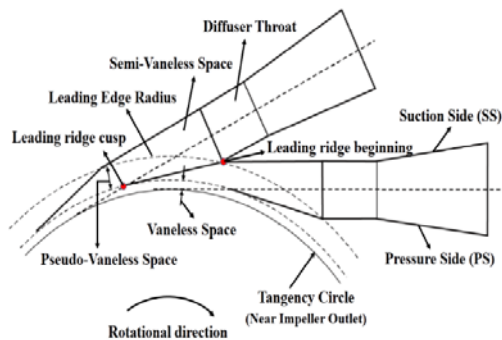


Fig. 2. Schematic of the pipe diffuser inlet region.

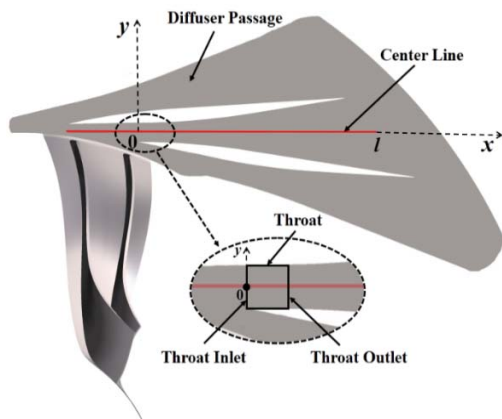


Fig. 3. Schematic of the diffuser passage and the reference frame.

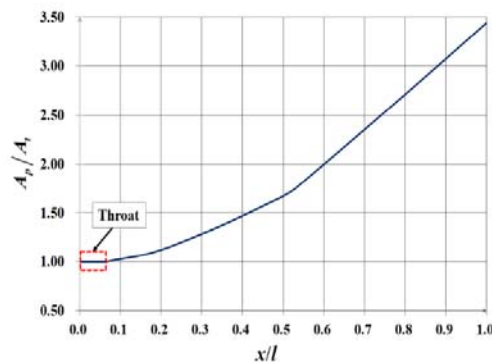


Fig. 4. Cross-section areas distribution along the center line of the diffuser passage.

3. SIMULATION MODEL AND VALIDATION

To investigate the detailed flow field of the pipe diffuser by numerical methods, a simulation model is established first. In this investigation, based on the three-dimensional steady compressible finite volume, the Reynolds-averaged Navier-Stokes equations are solved. Fourth order Runge-Kutta scheme and Central scheme are used for temporal discretization and spatial discretization, respectively. The Shear Stress Transport (SST) turbulence model is applied for turbulence closure. A multigrid procedure is applied to accelerate the convergence.

As for boundary conditions, the solid wall is set to be non-slip and adiabatic. Total pressure, total temperature as well as velocity directions are imposed as inlet boundary condition. Outlet conditions are changed depending on the operation condition. At near choke conditions, static pressure is imposed at the diffuser outlet while, at other conditions, averaged mass flow rate is imposed at the diffuser outlet. Besides, the frame change between the rotational impeller and stationary diffuser is achieved by the method of “Stage” supplied in ANSYS CFX, which is actually a method of “Full Non Matching Mixing Plane”.

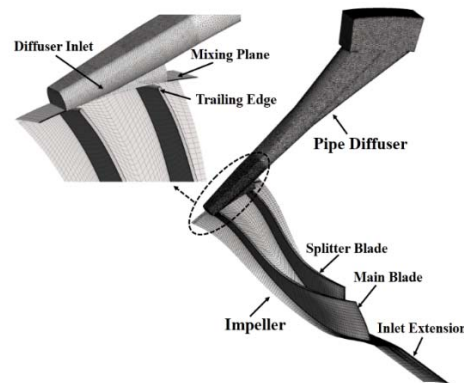


Fig. 5. The mesh of a single passage mesh in the compressor stage.

The impeller used in this investigation consists of 19 main blades and 19 splitter blades, and the pipe diffuser has 30 flow passages. The meshed domain only contains one single passage of the impeller and the pipe diffuser, which is adequate for the simulation requirements of this investigation. It is widely acknowledged that the spatial discretization error is directly related to the grid number. Usually, a higher grid number is needed for higher calculation accuracy, but it inevitably occupies more CPU time and storing memories. To determine the optimum grid number that can ensure both the accuracy and the acceptable time and memory requirements, several meshes with different grid numbers are tested. The results show that 500,000 nodes in a single impeller passage and 500,000 nodes in a pipe diffuser passage is a satisfying choice that meets all the simulation requirements. The mesh finally used is shown in

Fig. 5. For the impeller passage, a structured grid is created, and the mesh contains 546,819 nodes with 512,860 elements. For the pipe diffuser passage, there are 512,860 nodes, but more elements (2,080,072 elements) because an unstructured grid is used due to the complex geometry of the pipe diffuser. To get the suitable value of y^+ , the mesh height of the first layer is set as 0.001 mm, and seven prism layers are imposed near the pipe diffuser solid wall. As shown in Fig. 6, the y^+ for all solid wall is less than 3.0, which is an acceptable range for the application of SST turbulence model to obtain credible results (Vaughn *et al.* 2007).

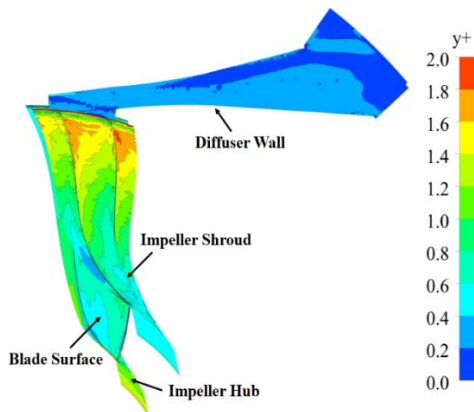


Fig. 6. Distribution of y^+ on all solid walls.

As the purpose of this paper lies not only on the overall stage performance of the compressor with a pipe diffuser, but also on certain details of the flow and interaction, it is appropriate to validate the numerical method at the level of both overall performance and detailed flow field. To do this, the overall and detailed experimental results of the compressor case “Radiver” is used to validate the accuracy of the simulation method. “Radiver” is a centrifugal compressor with wedge diffuser developed by the Institute of Jet Propulsion and Turbomachinery of the RWTH Aachen. The reason of selecting this compressor for numerical validation is because of abundant flow details inside this compressor obtained by advanced visual experiments. As for “Radiver”, the distance between wedge diffuser inlet and impeller outlet is adjustable, here we chose the results of case “ $r_{le} / r_{te} = 1.04$ ” for validation as this ratio almost equals to the ratio of the investigated pipe diffuser in this paper (r_{te} and r_{le} stands for the radius of impeller trailing edge and diffuser leading edge, respectively). Detailed introduction about the compressor “Radiver” and related experimental information could be found easily in published literatures (Ziegler *et al.* 2002, Ziegler *et al.* 2003, Weiß *et al.* 2003, and Ziegler 2003).

When simulating the case “Radiver”, the numerical model is set to be the same as the one used for the centrifugal compressor with pipe diffuser to ensure the scientificity of the

validation. The comparison between numerical and experimental total pressure ratio at 80% rotating speed is shown in Fig. 7. It can be seen that experimental and numerical results agree well in tendency as the largest relative difference is less than 5%, the CFD can predict the characteristics of the overall performance well despite the small flaw that the CFD underestimates the total pressure ratio slightly when the compressor operates at conditions near choke, while it overestimates the total pressure ratio slightly at near surge conditions.

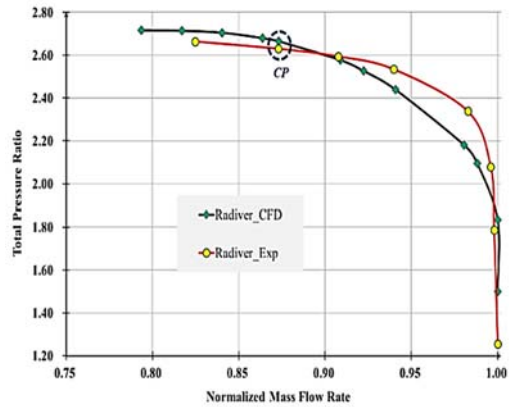


Fig. 7. Total pressure ratio comparison between experiment and CFD at 80% speed.

Two measurement locations named as 2M’ and 4M are selected to compare the detailed flow inside the compressor. As shown in Fig. 8, 2M’ locates near the outlet of the impeller and intersects with the trailing edge of the impeller blade, while the measurement plane 4M locates at the inlet of the wedge diffuser. The comparison in detailed flow is carried out at the similar operation condition marked as “CP” with a dash circle in Fig.7, where the mass flow rate is 87.5% of the choke mass flow rate, and the results of velocity comparison at 80% rotational speed are shown in Fig. 9 and Fig. 10.

According to Fig. 9, accurate prediction of the relative velocity at 2M’ measurement plane is obtained with CFD as the distribution of the magnitude of the relative velocity is quite similar between numerical and experimental results. It can be seen that the flow field at 2M’ is characterized by an area of low relative velocity near the shroud side, but this area is a little larger in the numerical result than that in the experimental result. In addition, high relative velocity areas are detected by both CFD and experiment at corners between the hub and the impeller blade. Obviously, the flow structure at 2M’ is of great agreement between CFD and experiment and the CFD method used in this paper is capable to catch the detailed flow in the impeller.

When it comes to measurement location 4M, the distribution of absolute velocity is compared between CFD and experiment. From Fig. 10 one can see that the numerical prediction of the flow field structure is again quite good. At areas near the

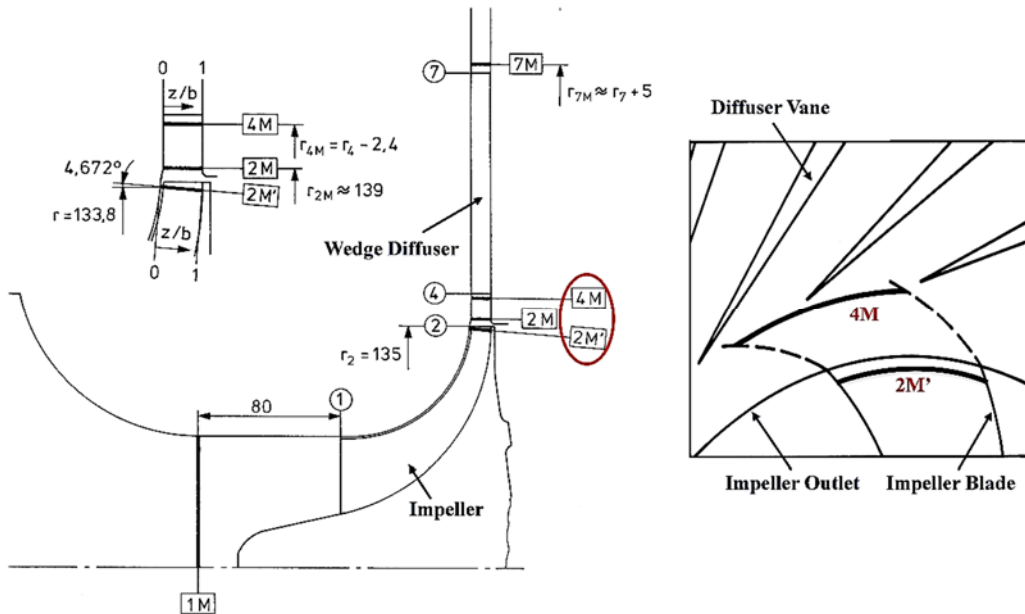


Fig. 8. Schematic of measurement locations in the compressor “Radiver” (Ziegler *et al.* 2003, and Ziegler 2003).

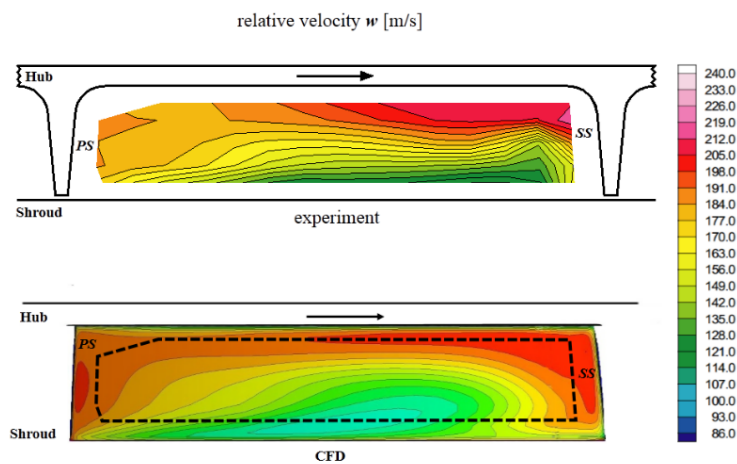


Fig. 9. Comparison of relative velocity at 2M' at the operating point “CP”.

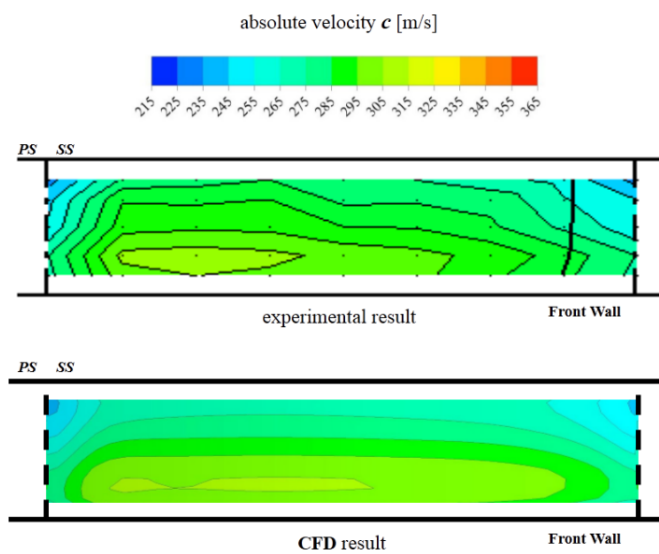


Fig. 10. Comparison of absolute velocity at 4M at the operating point “CP”.

leading edge of the wedge diffuser (marked by the vertical dash lines), low absolute velocity is shown by both numerical and experimental results, and high absolute velocity areas appear in the middle region between two adjacent diffuser vanes. Again the flow structure obtained by CFD and experiment at 4M shows great agreement, indicating the CFD can capture the main characteristics of the flow field.

The CFD results show a good agreement with the experimental results of the compressor “Radiver” in terms of overall stage performance and detailed flow field, especially the flow structure inside the impeller and diffuser. In spite of the acceptable small deviations in overall performance prediction (relative difference less than 5%), the numerical method is still capable to predict the overall performance and the main characteristics of the flow field. Therefore, it can be concluded that the numerical method used in this study is adequate for this investigation.

4. NUMERICAL RESULTS AND ANALYSIS

The stage performance and the inside flow of the investigated centrifugal compressor with a pipe diffuser are obtained by numerical methods. To study the relationship between the flow characteristics and the geometric features in the pipe diffuser, the operating condition of design speed is simulated, and the simulation results are shown from different aspects as follows.

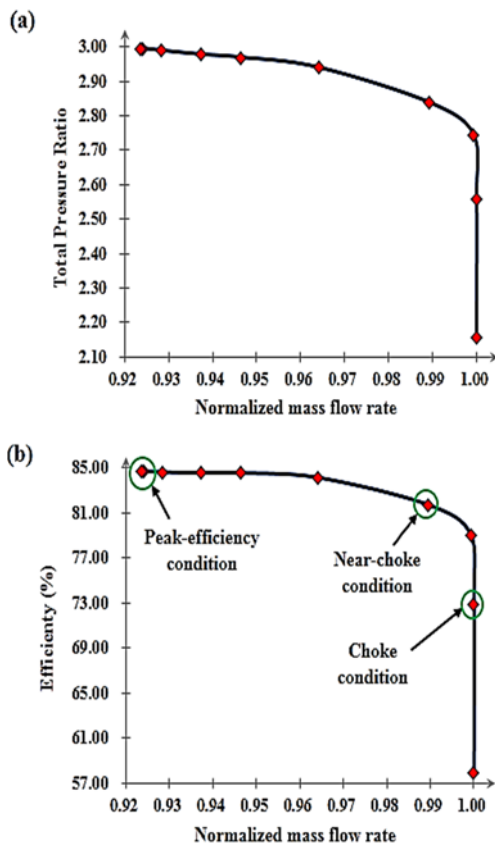


Fig. 11. Compressor map for (a) total pressure ratio and (b) isentropic efficiency.

4.1 Characteristics Related to Different Mass Flow Rates

The stage performance curve is one of the most significant characteristics of a compressor stage, from which a lot of useful information can be obtained immediately. Fig. 11 (a) and (b) show curves of total pressure ratio and isentropic efficiency versus normalized mass flow rate. Both two curves are steep when the normalized mass flow rate is nearly 1.0 (choke condition). Once the mass flow rate decreases slightly, however, the curves become flat immediately, and total pressure ratio and isentropic efficiency change slowly with further decrease in mass flow rate. This characteristic is quite different from that of conventional vaned diffusers or vaneless diffusers, and it indicates that the choke in the pipe diffuser happens suddenly. This characteristic is owed to the special geometric structure in the inlet region. At the upstream of the pipe diffuser throat, adjacent passages intersect in the inlet region and form sharp leading edges with elliptical ridges. This leading edge is a ‘swallow-tail’ type of geometry, and it allows the pipe diffuser to swallow a highly non-uniform flow (Cumpsty 2004, and Krain 2003). When the impeller discharge flow passing through the inlet region and arriving at the diffuser inlet, it becomes much more uniform. Therefore, at choke condition, most of the flow in the diffuser throat accelerates and reaches a speed of sound simultaneously, and when mass flow rate decreases, the pipe diffuser could free from the choke easily. Fig. 12 presents the Mach number distribution at the diffuser throat. The proportion of the throat area where the Mach number is less than 1.0 is no more than 20% at choke condition (Fig. 12 (a)), which means most of the flow passing the throat reaches the speed of sound simultaneously. However, at the near-choke condition (mass flow rate decreases by 1.0%), the Mach number at all the throat cross-section is less than 1.0 (Fig. 12 (b)), implying the pipe diffuser no longer suffers from the choke after a slight decrease in mass flow rate.

To investigate the characteristics of diffusion ability and loss generation in the pipe diffuser, the pressure recovery and the loss coefficient are used. These two parameters are defined as Eqs. (1) and (2). The definitions reveal that pressure recovery stands for the diffusion ability. Larger pressure recovery means more static pressure is obtained from decelerating the flow. Meanwhile, the loss coefficient represents the loss in total pressure, the smaller it is, the fewer losses are generated.

Pressure recovery:

$$c_p = \frac{p_2 - p_1}{p_{01} - p_1} \quad (1)$$

Loss coefficient:

$$\omega = \frac{p_{01} - p_{02}}{p_{01} - p_1} \quad (2)$$

The curves of loss efficient and pressure recovery for the investigated pipe diffuser are shown in Fig. 13 (a) and (b). With the decline of the normalized mass

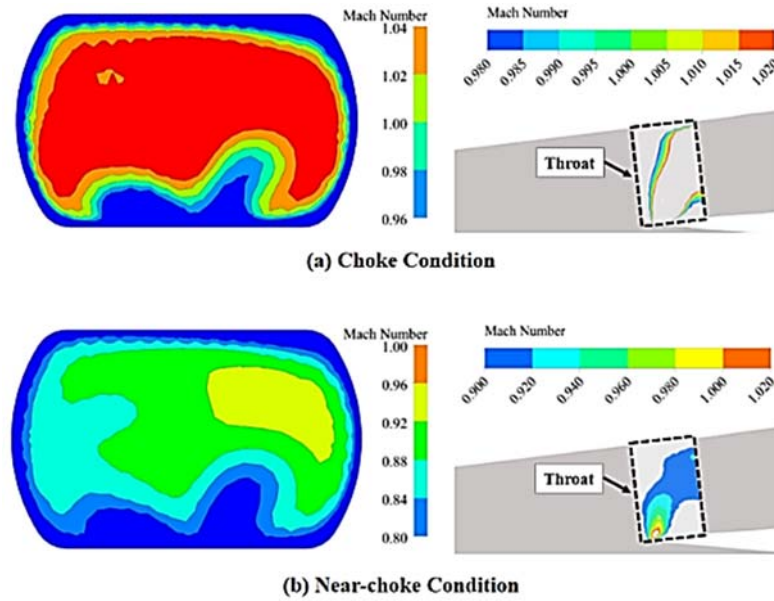


Fig. 12. Mach number at diffuser throat cross-section: (a) choke condition; (b) near-choke condition.

flow rate, the pressure recovery increases rapidly to a certain value, then slightly decreases. The loss coefficient presents an opposite tendency, as it decreases to a certain value and then slightly increases. According to Fig. 13 (a) and (b), 95% to 98% of the choke mass flow rate is an optimum operation flow range where the pipe diffuser can obtain high pressure recovery and low loss coefficient, which means obtaining high static pressure without generating high losses.

Stable flow range (SFR) is another important parameter of a compressor that stands for the stability. Its definition is expressed in Eq. (3)

$$SFR = \left(\frac{\dot{m}_{choke} - \dot{m}_{surge}}{\dot{m}_{choke}} \right)_{N=const} \times 100\% \quad (3)$$

where \dot{m}_{choke} and \dot{m}_{surge} are the mass flow rate at choke and surge point respectively. The SFR of the investigated pipe diffuser can be obtained from Fig. 11 and Fig. 13, and its value is near 8%. To ensure sufficient surge margin, the pipe diffuser should not operate at conditions near surge. So the suitable operating flow range for a pipe diffuser is suggested to be 96% to 98% of the choke mass flow rate. Within this flow range, the pipe diffuser could balance the static pressure rise, the loss generation, and the surge margin. Bennett *et al.* (2000) introduce a design criterion for the design of the diffuser throat size, he suggests that the design mass flow rate of the compressor stage should be 96% to 98% of the choke mass flow rate of the pipe diffuser. Therefore, when designing a pipe diffuser, it is better to set the throat to such a size that the mass flow rate of the design point is 96% to 98% of the choke mass flow rate.

4.2 Static Pressure Distribution along Diffuser Passage

The function of a diffuser is increasing the static

pressure by decelerating the high-speed flow discharged from the impeller outlet. The static pressure distribution along the flow passage is important for the diffuser performance. Regarding the diffuser passage as a one-dimensional flow channel, the reference frame shown in Fig. 2 can be used to display the static pressure distribution along the diffuser center line. The results of the investigated pipe diffuser are presented in Fig. 14. Obviously the distribution changes under different operating conditions.

Comparing the static pressure distribution at the choke condition and the peak-efficiency condition (both conditions are marked in Fig. 11), the biggest difference occurs in the throat region and the rear region (where $0 < x/l < 0.2$). As shown in Fig. 14 (a), the static pressure changes acutely in this region when the pipe diffuser operates at the choke condition. The static pressure decreases abruptly first and then increases sharply after the nadir which locates at the downstream of the throat where x/l is about 0.1. Nevertheless, the static pressure at the peak-efficiency condition increases smoothly at this region (shown in Fig. 14 (b)). The difference is mainly because of the incoming flow. According to the absolute Mach number distribution shown in Fig. 15, at the choke condition (Fig. 15 (a)) where the mass flow rate is relatively high, the flow accelerates to supersonic flow quickly when passing through the throat region. The supersonic flow continues to accelerate in the diffusion passage after the throat. Thus, the acceleration results in great and steep decrease in static pressure. Then the flow suffers a shock wave at the position where x/l is about 0.1. The shock wave heavily compresses the flow and increases the static pressure sharply. At the peak-efficiency condition (Fig. 15 (b)) where the mass flow rate is relatively low, the flow passing the passage is subsonic. Therefore, no supersonic acceleration or

shock wave appears, and no abrupt change happens in static pressure.

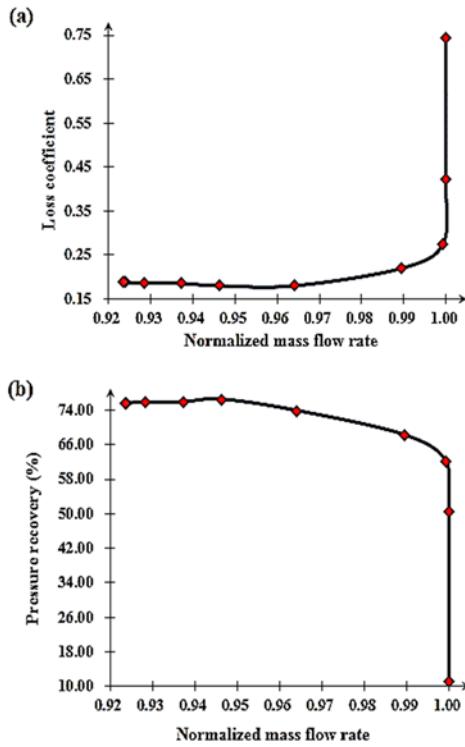


Fig. 13. Characteristics of (a) loss coefficient and (b) pressure recovery of the investigated pipe diffuser.

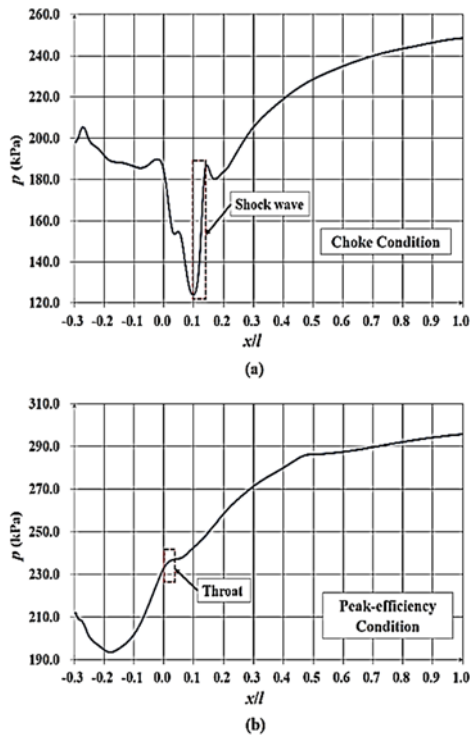


Fig. 14. Static pressure distribution along the diffuser passage center line at (a) choke condition and (b) peak-efficiency condition.

At both the choke condition and the peak-efficiency conditions, the static pressure increases more rapidly in the first half of the diffusion passage than the second half, and this can be verified from the slopes of the curves in Fig. 14. This is an inherent feature in a centrifugal diffuser, and some previous studies prove the reality. Zachau (2008) draws a similar conclusion from the experimental results in his investigation on the pipe diffuser, and Grates *et al.* (2014) present similar numerical and experimental results when investigating the static pressure distribution at the diffuser shroud. The increasing rate, however, cannot be too high, or the flow would suffer a great adverse static pressure gradient which exacerbates the instability of the flow field. So when designing a pipe diffuser, the increasing rate of the cross-section area of the diffusion passage is well controlled (shown in Fig. 4), especially at the first half of the passage. A pipe diffuser usually operates at 96% to 98% of the choke mass flow rate, indicating that the operating condition is close to the choke condition. At the first half of the passage, the absolute Mach number is close to 1.0, and a small change in cross-section area would cause a significant change in static pressure. The explanation is as follows.

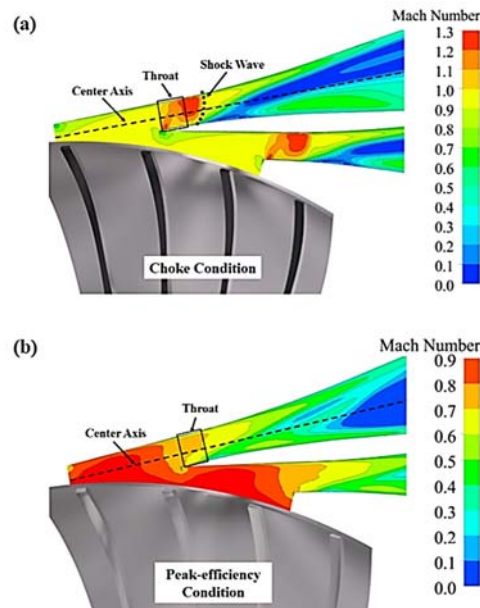


Fig. 15. Absolute Mach number distribution at 50% span at (a) choke condition and (b) peak-efficiency condition.

Regarding the diffuser passage as a pseudo one-dimensional heat-insulated pipe, and assuming that the flow inside is steady isentropic inviscid flow, a correlation can be expressed as Eq. (4).

$$(Ma^2 - 1) \frac{du}{u} = \frac{dA}{A} \Rightarrow \frac{du}{u} = \frac{1}{Ma^2 - 1} \frac{dA}{A} \quad (4)$$

where Ma denotes the local Mach number, u denotes the flow velocity along the center line, and A denotes the cross-section area of the diffuser passage.

According to Eq. (4), when Mach number is close

to 1.0, the velocity will change a lot with a small change in cross-section area, then great change occurs in the static pressure. So at the first half of the passage, the increasing rate of the cross-section area must be small to avoid an abrupt change in static pressure. Therefore, the cross-section area of the diffusion passage in a pipe diffuser increases slowly in the first half of the passage while increases much faster in the second half, as described in Fig. 4.

The first half of the diffusion passage of a pipe diffuser is significant as it has predominant influences on the performance of a pipe diffuser. The flow phenomena are complex here, shock wave and supersonic flow often occur, and the cross-section area determines the static pressure distribution. So it is recommended that improvement investigations should focus more on this area.

4.3 Vortices and Total Pressure Distribution

As mentioned in many publications (Gates *et al.* 2014, and Kunte *et al.* 2013), there is a pair of counter-rotating vortices inside the pipe diffuser passages, one is near the front wall (near impeller shroud) while the other one is near the back wall (near impeller hub), and this is a unique flow characteristic of the pipe diffuser. In this investigation, vortices are detected by steady simulation. To track their development in the flow direction, eight cross-sections of the diffuser passage are selected to display the shapes and locations of the two counter-rotating vortices. As exhibited in Fig. 16, these cross-sections are named from plane01 to plane08. Plane01 is located on the leading edge of the diffuser elliptical ridges while plane08 is close to the outlet of diffuser passage. Plane02 and plane03 locates at the throat inlet and outlet respectively.

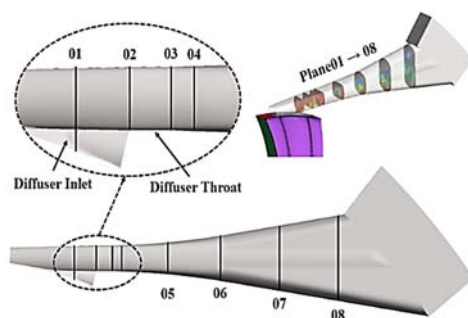


Fig. 16. Selected cross-sections in the pipe diffuser passage.

Streamline projections in these cross-sections are shown in Fig. 17 to illustrate the vortices. In plane01, the streamlines are greatly influenced by the elliptical ridges. The elliptical ridges function as a vortex generator in pipe diffusers. At the corner between the back wall and the PS, the velocity of the flow is low because of the passage expansion after the elliptical ridges, this flow interacts with the main flow passing over the elliptical ridges and generates the vortex near back wall. For the other vortex near the front wall, it can be greatly influenced by the elliptical ridges, but it has a different generation process. After leaving the impeller, the main flow

moves towards the suction side (SS). Because of the deflection effect of the passage wall, the main flow turns towards the front wall along SS, then it is redirected again near the front wall and moves towards the pressure side (PS) along the front wall. In this way, a vortex is generated near the front wall. This vortex also occurs in other radial bladed diffusers applied in centrifugal compressors. Ziegler *et al.* (2003) studied the unsteadiness of this vortex in a wedge-type diffuser, and Stahlecker *et al.* (1998) detected the vortex in a vaned diffuser by experimental methods. The vortex near the back wall can be seen clearly in plane02, implying that it is fully generated before entering the diffuser throat. After the elliptical ridge, the flow suffers an abrupt expansion and forms a backflow area at the corner between the back wall and the PS. The vortex near the back wall is generated by the interaction between the flow passing over the ridges and the flow in the backflow area. More detailed perspective about the generation process of the pair vortices is presented by Grates *et al.* (2014).

Besides the difference in locations and generations, the two vortices also differ in their sizes and moving trajectories. According to the streamlines in Fig. 17, both two vortices can be seen at the diffuser outlet, and the vortex near the front wall is larger than the one near the back wall in all eight planes. According to the streamlines from plane01 to plane08 shown in Fig. 17, the relative position of the two vortices varies at different locations. From diffuser inlet to outlet, the larger vortex moves from the front wall to the back wall, and is finally located in the middle area near the PS. Meanwhile, the smaller vortex moves from the PS to the SS along the back wall, and is finally located in the corner between the back wall and the SS.

The pair of vortices can affect the flow field inside the pipe diffuser significantly because they transform and redistribute the flow. Fig. 18 shows the total pressure distribution in different locations, and these distributions are directly related to this pair of vortices. At diffuser inlet regions (plane01 to plane04), the main flow from impeller outlet first rushes to SS, and then vortices shift it. As the vortex near the front wall is much larger and stronger, it plays a predominant role in shifting the flow. As a result, most of the high-momentum flow gathering near the SS is shifted by the larger vortex and moves towards the front wall along the SS. At regions further downstream, the larger vortex continues shifting the high-momentum flow from the SS to the PS along the front wall (from plane04 to plane08 in Fig. 18), and finally the high-momentum flow comes to the corner between the front wall and the PS. Meanwhile, the smaller vortex also transports some high-momentum flow from the SS to the PS along the back wall. As a result, high-momentum flow is brought to the PS by the pair of vortices and re-energizes the wake flow on the PS, thus reducing the aerodynamic loading. The vortices also shift wake flow to the center of the passage. In plane07 and plane08, an area filled with the low-momentum flow is clearly presented in the center regions.

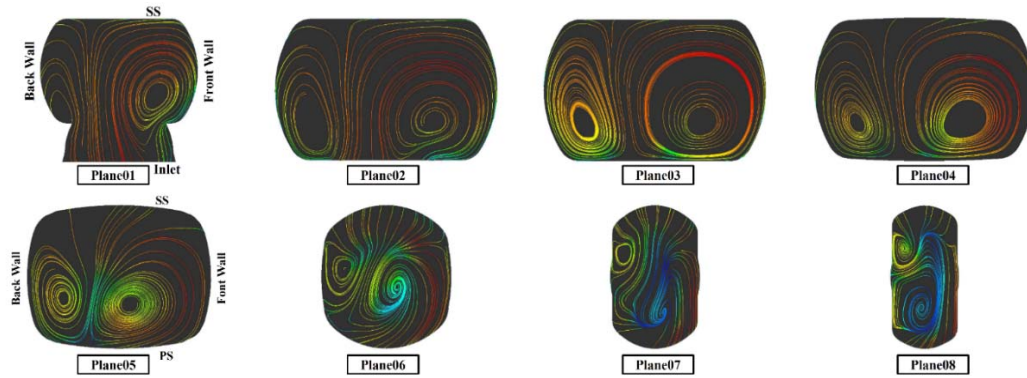


Fig. 17. Streamlines in different cross-sections at peak-efficiency condition (color stand for the amplitude of the flow velocity).

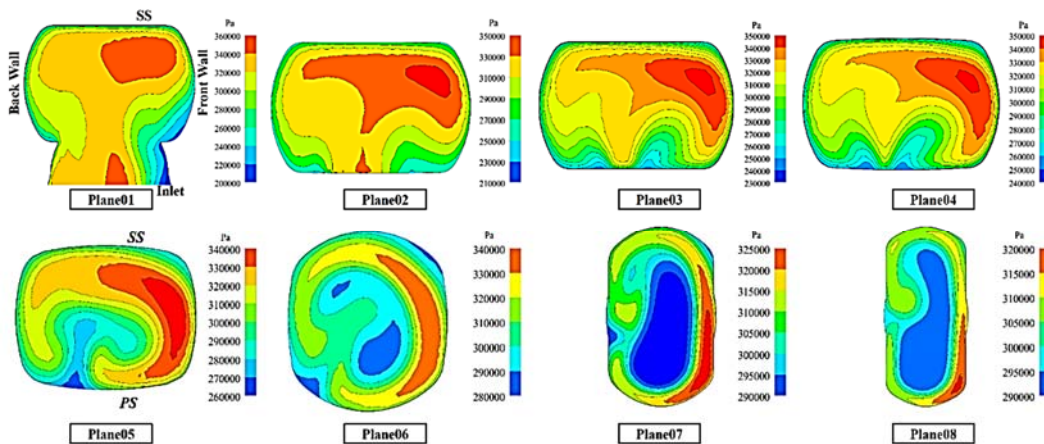


Fig. 18. Total pressure distribution in different cross-sections at peak-efficiency condition.

The transportation of flow by the pair vortices leads to two consequences: 1). A low-momentum flow cell is formed in the center area at the second half of the passage, and it is surrounded by an energy-rich flow-layer near the passage wall. 2). Boundary layer loading on the PS is reduced, and the flow stability is improved because the flow separation is suppressed on the PS by re-energizing the wake flow.

In fact, vortices are often used to control flow separation and improve the stability of compressors. For example, Hasegawa *et al.* (2008) study adaptive separation control system using vortex generator jets for time-varying flow and get some good results.

The pair of vortices is generated in the inlet region and they exist in the whole passage. By transferring the flow to certain positions, they can greatly influence the flow behavior and dominant the flow field, further influence the performance of the pipe diffuser. As the spatial structure of the inlet region, especially the structure of the elliptical ridges, has a great effect on the vortices in the process of improving the performance of the pipe diffuser, many works could be done on the elliptical ridges to control the vortices and improve the flow field.

4.4 Flow Separations

Flow separation in the pipe diffuser often occurs in the PS at the downstream of the diffuser throat (Zachau 2008) and is greatly affected by the vortices. Flow separation is much focused, especially at near surge conditions, because it affects both the stability and efficiency of the compressor stage. According to Fig. 11 (b), the peak-efficiency condition is very close to the surge line, so it is selected here to analyze the separated flow. To investigate the flow separation inside the pipe diffuser, four planes parallel to the front wall and the back wall are created, as shown in Fig. 19. The two planes near the back wall cut the pipe diffuser passages at 10% span and 30% span while the other two cut the pipe diffuser passages at 60% span and 90% span. As the flow separation is more likely to happen in areas where the flow momentum is low, the 30% span and the 60% span are of more possibility to detect flow separations because they interact with the wake flow cells in the diffuser passage (shown in Fig. 19).

Streamline projections in the four planes at peak-efficiency condition are shown in Fig. 20. According to the streamline distribution, flow separations happen near the PS at positions 1 and 2 in the 30% span and the 60% span, and streamlines tend to

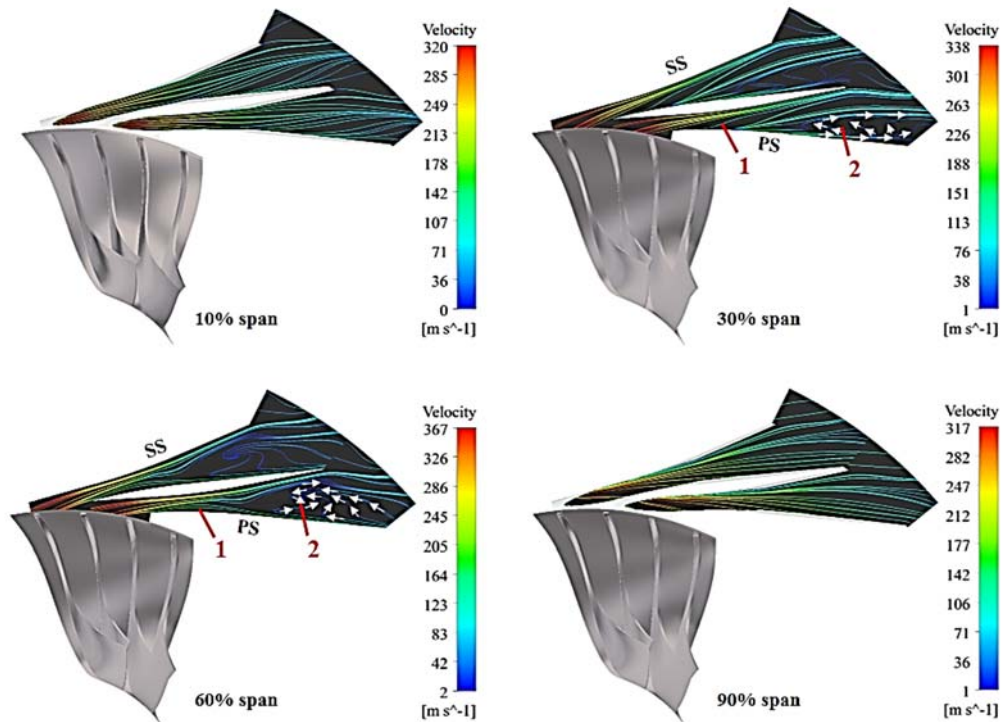


Fig. 20. Streamline projections in planes located in different spans (Peak-efficiency condition).

deflect towards the SS once separation occurs. The experimental results from Zachau (2008) present comparable flow phenomena. He studies the separation in different operating conditions and concludes that flow only separates near the PS in all investigated conditions. The flow separations are essentially related to the pair vortices generated in diffuser inlet region. As what has been mentioned when discussing the results in Fig. 18, the transportation effect of the two vortices redistributes the flow and forms wake flow cells in the diffuser passages. Position 1 and 2 at the 30% span and the 60% span are within or near these wake flow cells (Fig. 19), so the flow here is easier to separate.

There remains a difference between separations in position 1 and 2. Flow in position 2 is of low-momentum (see plane07 in Fig. 18) and suffers from heavy separation and reverse flow. By contrast, flow in position 1 separates slightly, and the separated flow even reattaches to the PS wall downstream at 60% span. In fact, the flow in position 1 is less likely to separate because its momentum is relatively higher, and the reverse static pressure gradient is well controlled by the passage expansion rate. It is the vortices that stimulate the slight separation. As shown in Fig. 21, the vortices shift flow from the PS to the SS in the 30% span and the 60% span, flow in position 1 is driven away from the PS wall. As a result, slight separation occurs here.

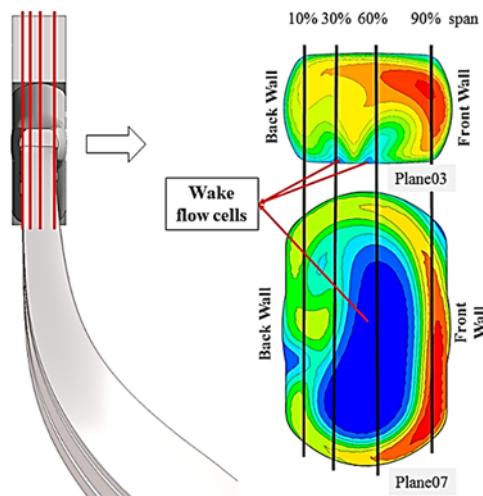


Fig. 19. Locations of planes parallel to the front wall and back wall.

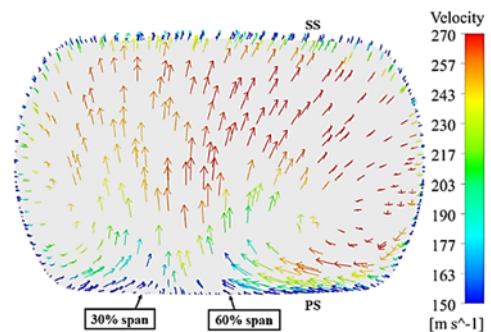


Fig. 21. Velocity vectors in plane04 at peak-efficiency condition.

Unlike at 30% and 60% span, no separation happens at 10% span and 90% span (Fig. 20), and this is the benefit of the vortices. Velocity vectors at plane04

(Fig. 21) show that vortices shift high-momentum flow from PS to SS along the front wall or the back wall, thus the wake flow near PS is re-energized and the boundary layer loading near the PS is reduced. In this way, the vortices improve the stability of the flow near the front wall and the back wall. Grates *et al.* (2014) also attribute the absence of flow separation in the front region of the PS to the transportation effects of the vortices.

In summary, it is obvious that the vortices have a dual effect on the flow separation in a pipe diffuser. Results from Zachau (2008) and results in Fig. 20 indicate that flow separations in pipe diffuser occur in the PS, so the separated flow moves from the PS towards the SS. According to Fig. 21, the vortices facilitate the flow separated from the PS at the middle regions of the passage, like 30% and 60% span. Meanwhile, it helps the flow to attach to the PS at regions near the back wall and the front wall, like 10% and 90% span. Therefore, such vortices are wanted, which can suppress the flow separation at near wall regions without greatly stimulating flow separation in the middle regions. So the inlet region and the elliptical ridges need to be carefully designed to obtain a pair of vortices that can balance both the two opposite sides.

5. CONCLUSIONS AND REMARKS

A three-dimensional numerical investigation has been carried out on a pipe diffuser to analyze the relationship between the flow characteristics and the geometric features. The following conclusions can be drawn from the results:

- (1) The pipe diffuser inlet region composed of the vaneless space, semi-vaneless space, and pseudo-vaneless space, is adaptable to high Mach number incoming flows. When passing the inlet region, the distorted flow from the impeller outlet becomes uniform. Thus, nearly all the flow at the diffuser throat moves at the speed of sound simultaneously, and the choke occurs suddenly. To obtain adequate surge margin as well as high efficiency, it is recommended that the mass flow rate at the design point of a pipe diffuser should be within 96% to 98% of the choke mass flow rate.
- (2) In a pipe diffuser, the cross-section area of the flow passages should increase slowly in the first half of the passage, which helps to gain an appropriate static pressure distribution. As the Mach number in the first half of a diffuser passage is relatively high, a slight increase in the cross-section area of the passage will result in a significant increase in the static pressure. Considering the great significant influence of the first half of the flow passage, it is suggested that improvement investigations should focus more on this region, especially the distribution of the area of the cross-section.
- (3) Numerical analysis shows that two counter-rotating vortices are generated in the diffuser inlet region, and they can exist in the downstream of the diffuser passage. They also

dominate the flow structure in the whole diffuser passages by shifting flows to certain locations and forming high-momentum flow cells and wake flow cells. Because the leading edge formed by the intersection of the adjacent diffuser passages significantly affects the generation of vortices, it is effective to optimize this region to control the vortices and improve the structure of the flow field.

- (4) The two counter-rotating vortices have suppression effect and facilitation effect on the flow separation in a pipe diffuser. Near the front wall and back wall, the vortices shift high-momentum flow from the suction side to the pressure side, and reduce aerodynamic loading on the pressure side and suppress the flow separation. However, they move the high-momentum flow away from the pressure side at center locations and facilitate the flow separation. In the process of designing a pipe diffuser, one of the key issues is to balance the suppression effect and the facilitation effect on the flow separation.

ACKNOWLEDGMENTS

This research is supported by the National Natural Science Foundation of China (Grant No. 51176087). Authors of this paper would like to give sincere appreciation to the Institute of Jet Propulsion and Turbomachinery of the RWTH Aachen for providing the test case "Radiver" whose experimental results are used to validate the CFD method in this investigation.

REFERENCES

- Bennett, I., A. Tournlidakis and R. L. Elder (1998). Detailed measurements within a selection of pipe diffusers for centrifugal compressors. In *Proceeding of ASME 1998 International Gas Turbine and Aeroengine Congress and Exhibition*.
- Bennett, I., A. Tournlidakis and R. L. Elder (2000). The design and analysis of pipe diffusers for centrifugal compressors. In *Proceedings of the Institution of Mechanical Engineers, Part A: Journal of Power and Energy* 214(1), 87-96.
- Cumpsty, N. A. (2004). *Compressor aerodynamics*. Kreiger Publishing Company, Malabar, FL.
- Grates, D. R., P. Jeschke and R. Niehuis (2014). Numerical investigation of the unsteady flow inside a centrifugal compressor stage with pipe diffuser. *Journal of Turbomachinery* 136(3).
- Groh, F. G., G. M. Wood, R. S. Kulp and D. P. Kenny (1970). Evaluation of a high hub/tip ratio centrifugal compressor. *Journal of Fluids Engineering* 92(3), 419-428.
- Han, G., X. Lu, S. Zhao, C. Yang and J. Zhu (2014). Parametric studies of pipe diffuser on performance of a highly loaded centrifugal compressor. *Journal of Engineering for Gas*

- Turbines and Power* 136(12).
- Hasegawa, H. and S. Kumagai (2008). Adaptive separation control system using vortex generator jets for time-varying flow. *Journal of Applied Fluid Mechanics* 1(2), 9-16.
- Kenny, D. P. (1969). A novel low-cost diffuser for high-performance centrifugal compressors. *Journal of Engineering for Gas Turbines and Power* 91(1), 37-46.
- Kenny, D. P. (1970). Supersonic radial diffusers. *Advanced Compressors (AGARD Lecture Series, Vol. 39)*, Brussels, Belgium.
- Kenny, D. P. (1972). A comparison of the predicted and measured performance of high pressure ratio centrifugal compressor diffusers. In *Proceeding of ASME 1972 International Gas Turbine and Fluids Engineering Conference and Products Show*.
- Krain, H. (2003). Review of centrifugal compressor's application and development. In *Proceeding of ASME Turbo Expo 2003, Collocated with the 2003 International Joint Power Generation Conference* 43-53.
- Kunte, R., P. Jeschke and C. Smythe (2013). Experimental investigation of a truncated pipe diffuser with a tandem deswirl in a centrifugal compressor stage. *Journal of Turbomachinery* 135(3).
- Kunte, R., P. Schwarz, B. Wilkosz, P. Jeschke and C. Smythe (2013). Experimental and numerical investigation of tip clearance and bleed effects in a centrifugal compressor stage with pipe diffuser. *Journal of Turbomachinery* 135(1).
- Reeves, G. B. (1977). Design and performance of selected pipe-type diffusers. In *Proceeding of Gas Turbine Conference and Products Show*, Philadelphia.
- Runstadler, P. W. and R. C. Dean (1969). Straight channel diffuser performance at high inlet mach numbers. *Journal of Fluids Engineering* 91(3), 397-412.
- Salvage, J. W. (1997). Variable geometry pipe diffusers. *Journal of Turbomachinery* 119(4), pp. 831-838.
- Stahlecker, D., E. Casartelli and G. Gyarmathy (1998). Secondary flow field measurements with a ldv in the vaned diffuser of a high-subsonic centrifugal compressor. In *Proceeding of 9th International Symposium on Application of Laser Techniques to Fluid Mechanics*, Lisbon, Portugal 13-16.
- Vaughn, M. and C. Chen (2007). Error versus y^+ for three turbulence models: incompressible flow over a unit flat plate. *AIAA Paper*, 3968.
- Weiß, C., D. R. Grates, H. Thermann and R. Niehuis (2003, January). Numerical investigation of the influence of the tip clearance on wake formation inside a radial impeller. In *ASME Turbo Expo, collocated with the 2003 International Joint Power Generation Conference* (681-691), American Society of Mechanical Engineers.
- Zachau, U. (2008). *Experimental investigation on the diffuser flow in a centrifugal compressor with pipe diffuser*. Ph. D. thesis, RWTH Aachen, Aachen.
- Zachau, U., R. Niehuis, H. Hoenen and D. C. Wisler (2009). Experimental investigation of the flow in the pipe diffuser of a centrifugal compressor stage under selected parameter variations. *ASME Turbo Expo 2009: Power for Land, Sea, and Air* 1213-1223.
- Ziegler, K. U. (2003). *Experimental investigation of impeller-diffuser interaction in a centrifugal compressor of variable geometry*. Ph. D. thesis, RWTH Aachen, Aachen, Germany.
- Ziegler, K. U., H. E. Gallus and R. Niehuis (2002, January). A study on impeller-diffuser interaction: part I — influence on the performance. In *Proceeding of ASME Turbo Expo: Power for Land, Sea, and Air* (545-556), American Society of Mechanical Engineers.
- Ziegler, K. U., H. E. Gallus and R. Niehuis (2003). A study on impeller-diffuser interaction: part II — detailed flow analysis. *Journal of Turbomachinery* 125(1), 183-192.